Brief Report

Cone and Rod Loss in Stargardt Disease Revealed by Adaptive Optics Scanning Light Ophthalmoscopy

Hongxin Song, PhD; Ethan A. Rossi, PhD; Lisa Latchney, MS; Angela Bessette, MD; Edwin Stone, MD, PhD; Jennifer J. Hunter, PhD; David R. Williams, PhD; Mina Chung, MD

IMPORTANCE Stargardt disease (STGD1) is characterized by macular atrophy and flecks in the retinal pigment epithelium. The causative *ABCA4* gene encodes a protein localizing to photoreceptor outer segments. The pathologic steps by which *ABCA4* mutations lead to clinically detectable retinal pigment epithelium changes remain unclear. We investigated early STGD1 using adaptive optics scanning light ophthalmoscopy.

OBSERVATIONS Adaptive optics scanning light ophthalmoscopy imaging of 2 brothers with early STGD1 and their unaffected parents was compared with conventional imaging. Cone and rod spacing were increased in both patients ($P < .001$) with a dark cone appearance. No foveal cones were detected in the older brother. In the younger brother, foveal cones were enlarged with low density (peak cone density, 48.3×10^3 cones/mm^2). The ratio of cone to rod spacing was increased in both patients, with greater divergence from normal approaching the foveal center, indicating that cone loss predominates centrally and rod loss increases peripherally. Both parents had normal photoreceptor mosaics. Genetic testing revealed 3 disease-causing mutations.

CONCLUSIONS AND RELEVANCE This study provides in vivo images of rods and cones in STGD1. Although the primary clinical features of STGD1 are retinal pigment epithelial lesions, adaptive optics scanning light ophthalmoscopy reveals increased cone and rod spacing in areas that appear normal in conventional images, suggesting that photoreceptor loss precedes clinically detectable retinal pigment epithelial disease in STGD1.

+ Supplemental content at jamaophthalmology.com

Author Affiliations: Center for Visual Science, University of Rochester, Rochester, New York (Song, Rossi, Hunter, Williams, Chung); Flaum Eye Institute, University of Rochester, Rochester, New York (Latchney, Bessette, Chung); Department of Ophthalmology and Visual Sciences, Carver College of Medicine, Iowa City, Iowa (Stone); Stephen A. Wynn Institute for Vision Research, University of Iowa, Iowa City (Stone); Howard Hughes Medical Institute, University of Iowa, Iowa City (Stone); The Institute of Optics, University of Rochester, Rochester, New York (Hunter, Williams).

Corresponding Author: Mina Chung, MD, Flaum Eye Institute, University of Rochester, 601 Elmwood Ave, PO Box 659, Rochester, NY 14642 (mina_chung@urmc.rochester.edu).

Stargardt disease (STGD1) is characterized by macular atrophy and peripheral flecks in the retinal pigment epithelium (RPE). The causative gene, *ABCA4* (OMIM 601691),[1] encodes a protein localizing to photoreceptor outer segments[2] that transports vitamin A byproducts across the disc membrane.[3] Loss of ABCA4 function is associated with RPE lipofuscin accumulation[4] and photoreceptor degeneration in mouse models. A pathogenic sequence of lipofuscin accumulation leading to RPE cell damage and then photoreceptor loss has been proposed.[5]

Mutations of *ABCA4* are associated with a spectrum of phenotypes, including cone-rod dystrophy and retinitis pigmentosa.[6] Several hundred sequence variations in *ABCA4* have been identified.[7,8] Assessment of the pathogenic contribution of disease-causing alleles has indicated the presence of non-*ABCA4* modifying factors.[9] Given the phenotypic variability of *ABCA4*-associated disease, predicting its spatial and temporal progression is critical for the development of potential therapies.[10]

Conventional imaging has been useful to characterize STGD1. Fundus autofluorescence (FAF) shows early diffuse lipofuscin accumulation, hyper-AF within flecks, and hypo-AF indicating RPE atrophy.[11] Optical coherence tomography (OCT) shows thickening of the foveal external limiting membrane, suggesting early gliosis.[12] These methods remain limited by the eye's optical irregularities.

Adaptive optics scanning light ophthalmoscopy (AOSLO) enables visualization of single photoreceptor cells in the living human retina, including foveal cones and peripheral rods.[13] Diseased photoreceptors can be measured quantitatively, and cone loss has been shown[14] to correlate with clinically identified lesions in STGD1. To investigate early STGD1, we used AOSLO to evaluate 2 brothers with macular atrophy, a mild phenotype, and their unaffected parents.

Methods

Clinical Examination

Complete ophthalmic examinations, fundus photographs (FF450*plus*; Carl Zeiss Meditec Inc), and spectral-domain OCT and FAF (Spectralis OCT and Heidelberg Regina Angiograph; Heidelberg Engineering) were obtained. The University of Rochester Research Subjects Review Board approved this study. Written informed consent was obtained and participants received financial compensation.

Molecular Genetics

Participants' DNA was tested for mutations in *ABCA4*. Sequence variations were evaluated as disease causing by using standard techniques.[7]

AOSLO Imaging

Cone and rod photoreceptor images were acquired using the Rochester AOSLO technique (eMethods in the Supplement). Photoreceptors were labeled semiautomatically. A foveal cone density map was generated and peak cone density was measured. The center of the foveal avascular zone and the preferred retinal locus were identified. Photoreceptor spacing was compared with normative AOSLO or histologic data[15] using 1-way analysis of variance with Bonferroni correction.

Results

Clinical Data and Molecular Genetics

Two brothers with STGD1 and their unaffected parents, both in their 40s, were examined. The older brother (II-1) had 20/150 Snellen visual acuity with a central scotoma. The younger brother (II-2) had 20/30 Snellen visual acuity. The father (I-1) and mother (I-2) had normal visual acuity. Molecular genetic analysis revealed 3 disease-causing *ABCA4* mutations: Gly1961Glu (paternal allele) and Gly863Ala and Arg2030Stop (maternal allele).

Clinical Imaging

Both parents' fundus, OCT, and FAF images were normal (**Figure 1A**-C). One son (II-1) showed macular atrophy with no peripheral flecks. Optical coherence tomography confirmed atrophy of the outer retina, RPE at the fovea, and normal layers at 1.7 mm. Fundus autofluorescence indicated central hypo-AF, surrounding hyper-AF at 0.7 mm, and uniform AF at 1.7 mm (Figure 1A-C).

The other son (II-2) had a subtle bull's-eye maculopathy with no peripheral flecks. Optical coherence tomography showed foveal preservation of the outer segments with a thickened external limiting membrane, perifoveal atrophy of the outer retina and RPE, and normal layers at 1.7 mm. Fundus AF indicated a bull's-eye with central hyper-AF, and surrounding annular hypo-AF, then hyper-AF at 0.7 mm. Autofluorescence was uniform at 1.7 mm (Figure 1A-C).

At a Glance

- To investigate the pathologic sequence of Stargardt disease, we used adaptive optics scanning light ophthalmoscopy (AOSLO) to examine the cones and rods in 2 brothers with early macular atrophy.
- AOSLO revealed increased cone and rod spacing in areas that appeared normal in conventional images, suggesting that photoreceptor loss precedes clinically detectable retinal pigment epithelium disease.
- Early pathologic features detected by AOSLO included a decline in peak foveal cone density and enlarged photoreceptor size.
- The presence of dark cones suggests foreshortened outer segments that may indicate potential target areas for therapy.
- Both parents, genetically confirmed carriers of disease-causing mutations in *ABCA4*, had normal photoreceptor mosaics.

Photoreceptor Structure

Both parents' photoreceptor mosaics were normal (Figure 1D-F). Cones were continuous and densely packed at the fovea, with increased spacing eccentrically. At 1.7 mm, rods were identified, but rod spacing could not be measured reliably owing to dense packing and the more limited resolution for rods at the wavelength and pinhole settings used.

At the fovea, no cones were identifiable in patient II-1 (Figure 1D). In patient II-2, foveal cones were sparse and enlarged, with a surrounding annulus of no identifiable cones (Figure 1D and Figure 2A). Peak cone density measured 48.3×10^3 cones/mm² (normal, 199×10^3 cones/mm² $\pm$ 87×10^3 cones/mm²). The locations of peak cone density, foveal avascular zone center, and preferred retinal locus were within 50 μm (Figure 2B).

Eccentrically, photoreceptors were qualitatively similar for patients II-1 and II-2. At 0.7 mm, cones were sparse, and cone spacing could not be measured reliably owing to the absence of a continuous mosaic (Figure 1E). At 1.7 mm, cones were abnormally dark, enlarged, and sparse; individual rods were identified and quantifiable (Figure 1F; Figure 2C and D).

Photoreceptor Spacing

Both parents' cone spacing was normal at all locations measured. In both affected brothers, cone spacing was increased and was worse in patient II-1 ($P < 10^{-6}$). Rod spacing was also increased and was worse in patient II-1 ($P = .048$), diverging further from normal with increasing eccentricity. The ratio of cone to rod spacing was increased, again worse in patient II-1 ($P < 10^{-6}$), and was most divergent from normal at lower eccentricities (**Figure 3**).

Discussion

Although cone loss has been shown[14] to correlate with clinically identified lesions in STGD1, in this study, in vivo AOSLO imaging of both rods and cones revealed several patterns of photoreceptor disease that are not detectable by conventional imaging methods. Although both affected individuals manifested macular atrophy without flecks, photoreceptor

Figure 1. Multimodal Imaging of the Father (I-1), Mother (I-2), and Patients (II-1 and II-2)
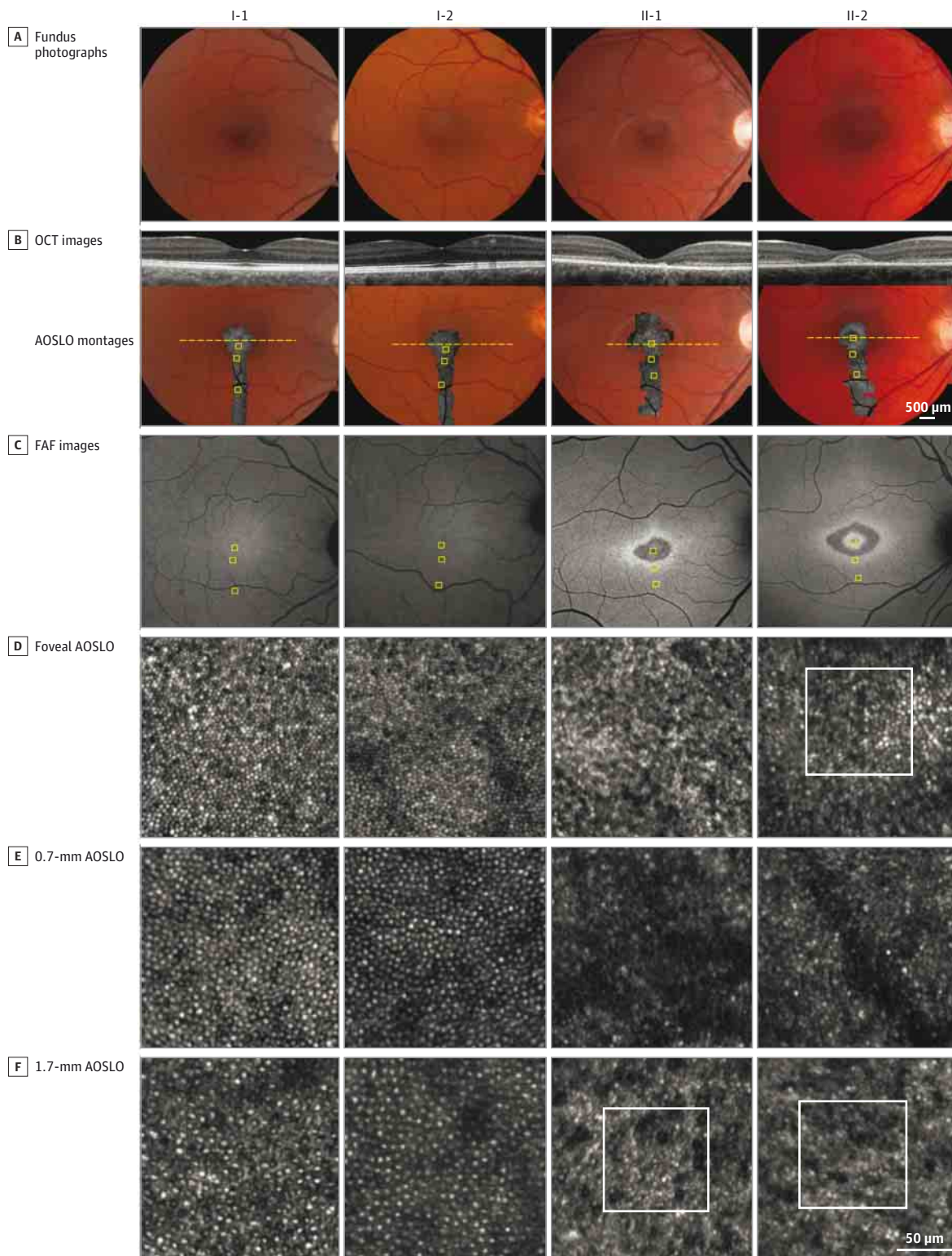
A, Fundus photographs. B, In the adaptive optics scanning light ophthalmoscopic (AOSLO) montages superimposed on fundus photographs, the dotted lines indicate the locations of the optical coherence tomographic images above. Yellow squares (B and C) indicate the AOSLO locations shown in D through F. The boxes (D and F) indicate the locations of AOSLO images shown at higher magnification in **Figure 2**. The scale bar in the AOSLO montage for patient II-2 applies to all of the fundus photographs, and the scale bar in the 1.7-mm AOSLO image for the same patient applies to all of the AOSLO images (D-F). FAF indicates fundus autofluorescence.

Figure 2. Photoreceptor Labeling

A Patient II-2

B Patient II-2, cone density map
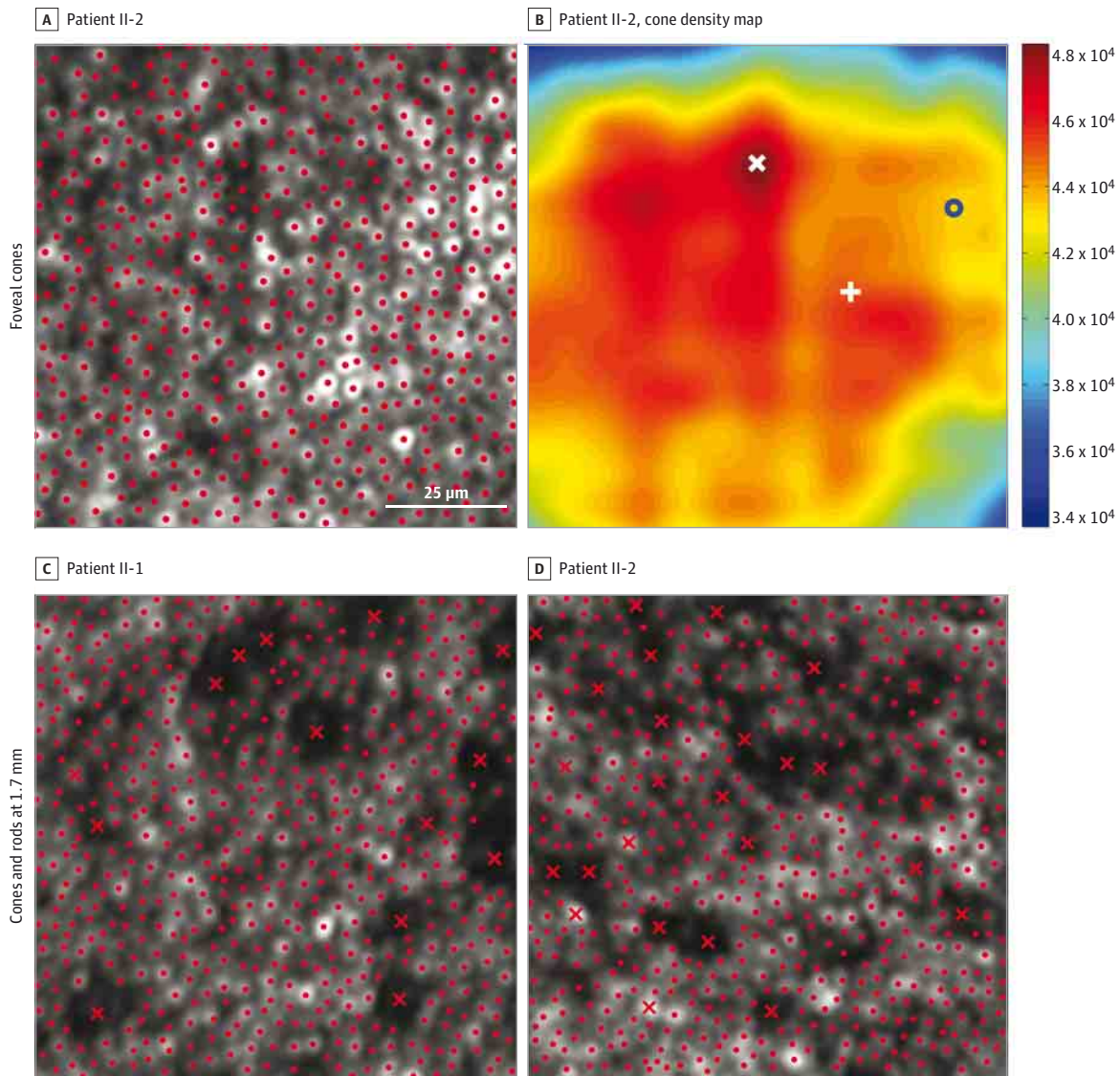
The adaptive optics scanning light ophthalmoscopic image locations (A, C, and D) correspond to the boxes in Figure 1D and F. A, Red dots indicate foveal cones. B, Open circle indicates the foveal avascular zone center; X, peak cone density; and +, preferred retinal locus. C and D, x indicates cones; red dots, rods.

spacing was significantly increased peripheral to the clinically detectable lesions. Fundus autofluorescence is homogeneous at these locations, suggesting that a decline in photoreceptors precedes lipofuscin accumulation in the macular atrophy phenotype. The finding that increased photoreceptor spacing was greater in the older brother with more advanced disease lends further credence to the hypothesis that photoreceptor loss represents an early step in the pathogenic sequence. Further investigation, including longitudinal follow-up and fluorescence AOSLO, is needed to confirm this interpretation.

In patient II-2, peak foveal cone density measured approximately 25% of the normal mean, consistent with a previous report[14] describing increased cone spacing near the fovea in STGD1. The foveal cones were continuous and larger than nor-

mal. At 1.7 mm in both patients, rods were similarly continuous with increased spacing. Whether photoreceptors enlarge and migrate to fill gaps where cells have died or whether fewer photoreceptors are present at birth in STGD1 remains unknown.

The ratio of cone to rod spacing was increased, with greater divergence from normal approaching the fovea, suggesting that cone loss predominates centrally and rod loss increases peripherally. In patient II-2, the locations of peak cone density, preferred retinal locus, and foveal avascular zone center did not overlap but were within normal range. The divergence of these points may be useful to monitor early foveal disease.

Peripherally, cone reflectance was diminished, producing a dark appearance. The presence of dark cones has been described[16-19] in other retinal degenerations and may repre-

Figure 3. Photoreceptor Spacing
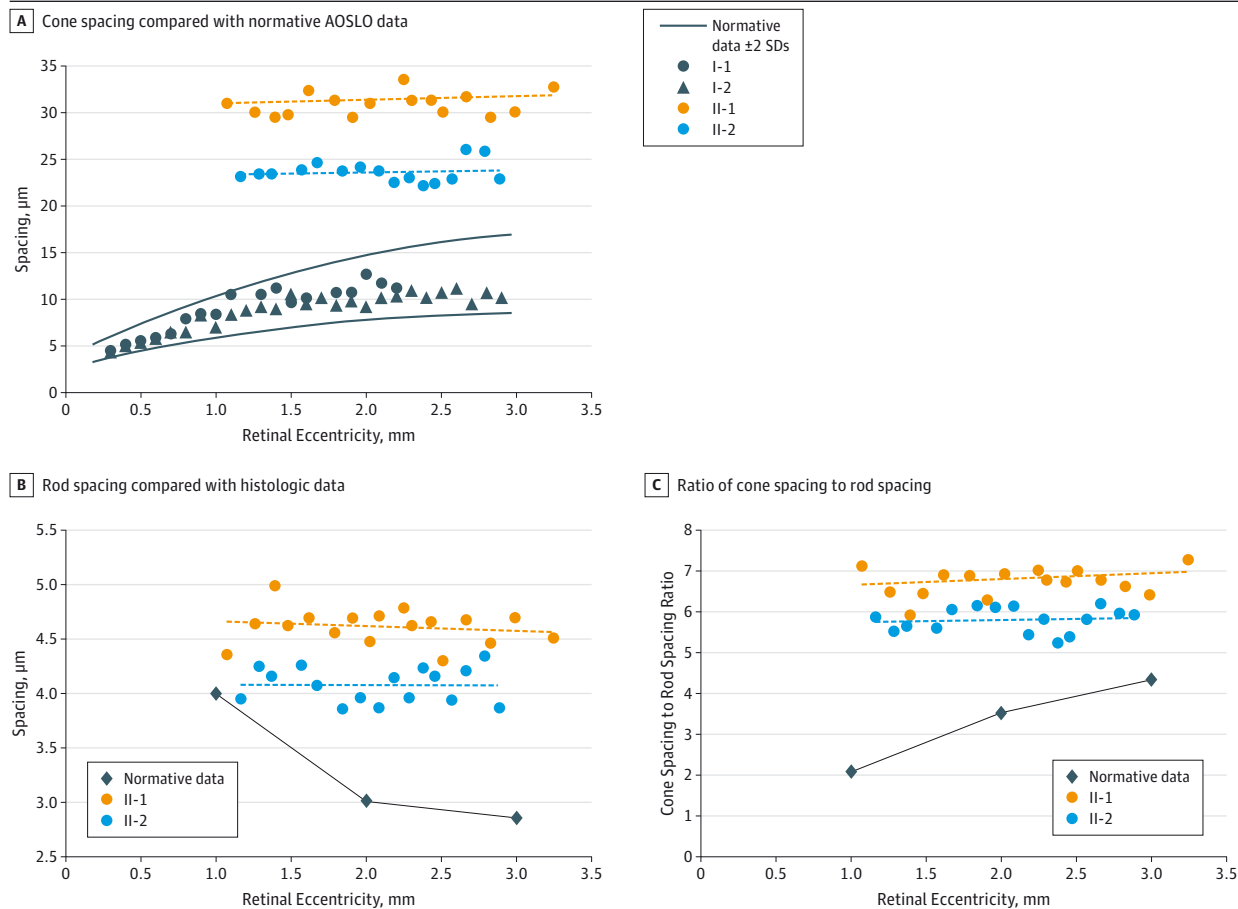
AOSLO indicates adaptive optics scanning light ophthalmoscopy; dashed lines, exponential fit curves for patients II-1 and II-2.

sent foreshortened outer segments. Nonconfocal split-detector AOSLO has shown[16] intact inner segments underlying dark cones, which may indicate potential targets for treatment, such as gene therapy.

Two of the 3 disease-causing mutations—Gly1961Glu (paternal) and Gly863Ala (maternal)—have been associated with a milder visual acuity and visual field phenotype.[9] The additional Arg2030Stop mutation on the maternal allele is uncommon, and its pathogenic contribution has not been well described, but the 2 mutations on the maternal allele were not sufficient to cause disease in the carrier state.

Conclusions

Adaptive optics scanning light ophthalmoscopy reveals increased cone and rod spacing in regions outside of the clinically detectable RPE changes in the macular atrophy phenotype of STGD1. Cone loss predominates closer to the fovea, with a greater contribution from rod loss in the periphery. Dark cones may indicate areas of outer-segment loss with preserved inner segments, suggesting potential therapeutic targets.

REFERENCES

1. Allikmets R, Singh N, Sun H, et al. A photoreceptor cell-specific ATP-binding transporter gene (ABCR) is mutated in recessive Stargardt macular dystrophy. *Nat Genet*. 1997;15(3): 236-246.

2. Sun H, Nathans J. Stargardt's ABCR is localized to the disc membrane of retinal rod outer segments. *Nat Genet*. 1997;17(1):15-16.

3. Sun H, Molday RS, Nathans J. Retinal stimulates ATP hydrolysis by purified and reconstituted ABCR, the photoreceptor-specific ATP-binding cassette transporter responsible for Stargardt disease. *J Biol Chem*. 1999;274(12):8269-8281.

4. Weng J, Mata NL, Azarian SM, Tzekov RT, Birch DG, Travis GH. Insights into the function of Rim protein in photoreceptors and etiology of Stargardt's disease from the phenotype in abcr knockout mice. *Cell*. 1999;98(1):13-23.

5. Cideciyan AV, Aleman TS, Swider M, et al. Mutations in ABCA4 result in accumulation of lipofuscin before slowing of the retinoid cycle: a reappraisal of the human disease sequence. *Hum Mol Genet*. 2004;13(5):525-534.

6. Cremers FPM, van de Pol DJR, van Driel M, et al. Autosomal recessive retinitis pigmentosa and cone-rod dystrophy caused by splice site mutations in the Stargardt's disease gene ABCR. *Hum Mol Genet*. 1998;7(3):355-362.

7. Stone EM, Webster AR, Vandenburgh K, et al. Allelic variation in ABCR associated with Stargardt disease but not age-related macular degeneration. *Nat Genet*. 1998;20(4):328-329.

8. Zernant J, Xie YA, Ayuso C, et al. Analysis of the ABCA4 genomic locus in Stargardt disease. *Hum Mol Genet*. 2014;23(25):6797-6806.

9. Schindler EI, Nylen EL, Ko AC, et al. Deducing the pathogenic contribution of recessive ABCA4 alleles in an outbred population. *Hum Mol Genet*. 2010;19(19):3693-3701.

10. Cideciyan AV, Swider M, Aleman TS, et al. ABCA4 disease progression and a proposed strategy for gene therapy. *Hum Mol Genet*. 2009;18 (5):931-941.

11. Lois N, Halfyard AS, Bird AC, Holder GE, Fitzke FW. Fundus autofluorescence in Stargardt macular dystrophy–fundus flavimaculatus. *Am J Ophthalmol*. 2004;138(1):55-63.

12. Lee W, Nõupuu K, Oll M, et al. The external limiting membrane in early-onset Stargardt disease. *Invest Ophthalmol Vis Sci*. 2014;55(10):6139-6149.

13. Dubra A, Sulai Y. Reflective afocal broadband adaptive optics scanning ophthalmoscope. *Biomed Opt Express*. 2011;2(6):1757-1768.

14. Chen Y, Ratnam K, Sundquist SM, et al. Cone photoreceptor abnormalities correlate with vision loss in patients with Stargardt disease. *Invest Ophthalmol Vis Sci*. 2011;52(6):3281-3292.

15. Song H, Chui TY, Zhong Z, Elsner AE, Burns SA. Variation of cone photoreceptor packing density with retinal eccentricity and age. *Invest Ophthalmol Vis Sci*. 2011;52(10):7376-7384.

16. Kim JE, Chung M. Adaptive optics for retinal imaging: current status. *Retina*. 2013;33(8): 1483-1486.

17. Song H, Latchney L, Williams D, Chung M. Fluorescence adaptive optics scanning laser ophthalmoscope for detection of reduced cones and hypoautofluorescent spots in fundus albipunctatus. *JAMA Ophthalmol*. 2014;132(9): 1099-1104.

18. Genead MA, Fishman GA, Rha J, et al. Photoreceptor structure and function in patients with congenital achromatopsia. *Invest Ophthalmol Vis Sci*. 2011;52(10):7298-7308.

19. Scoles D, Sulai YN, Langlo CS, et al. In vivo imaging of human cone photoreceptor inner segments. *Invest Ophthalmol Vis Sci*. 2014;55(7): 4244-4251.